Hexaazamacrocycle Containing Pyridine and Its Dicopper Complex as Receptors for Dicarboxylate Anions

Feng Li,[a] Rita Delgado,*[a,b] and Vítor Félix[c]

Keywords: Hexaazamacrocycle / Dicarboxylate anion recognition / Cascade dicopper complexes / Molecular dynamics / Receptors

The host–guest binding interactions of the hexaazamacrocycle [26]py_2N_4, in its tetraprotonated form H_4[26]$py_2N_4^{4+}$ as well as in its dicopper(II) complex $[Cu_2([26]py_2N_4)(H_2O)_4]^{4+}$, with dicarboxylate anions of different stereoelectronic requirements, such as oxalate (ox^{2-}), malonate (mal^{2-}), succinate (suc^{2-}), fumarate (fu^{2-}) and maleate (ma^{2-}), were evaluated. The association constants were determined using potentiometric methods in aqueous solution, at 298.0 K and 0.10 mol·dm^{-3} KCl. These values for the tetraprotonated ditopic receptor with the dicarboxylate anions revealed that the main species in solution corresponds to the formation of $\{H_4[26]py_2N_4(A)\}^{2+}$ (pH ≈ 4–9), A being the substrate anion. The values determined are not especially high, but the receptor exhibits selectivity for the malonate anion. The study of the cascade complexes revealed several species in solution, involving mononuclear and dinuclear complexes, mainly protonated and hydrolysed species, as well as the expected complexes $[Cu_2([26]py_2N_4)(A)(H_2O)_x]^{2+}$ or $[Cu_2([26]py_2N_4)(A)_2(H_2O)_y]$. Ox^{2-} and mal^{2-} form cascade complexes with only one anion, which will necessarily bridge the two copper atoms because of the symmetrical arrangement of the dinuclear complex. The two other studied anions, suc^{2-} and ma^{2-}, form species involving two substrate anions, although species with only one suc^{2-} anion were also found. UV/Vis and EPR spectroscopy have shown that the dicopper complex can operate as a sensor to detect and quantitatively determine oxalate spectrophotometrically because of the red shift of the maximum of the visible band observed by addition of ox^{2-} to an aqueous solution of the dinuclear copper complex. However the selectivity of $[Cu_2([26]py_2N_4)(H_2O)_4]^{4+}$ as a receptor for ox^{2-} in the studied series is not sufficiently high to detect ox^{2-} spectrophotometrically in the presence of the other anions. Molecular dynamics simulations indicated that the $H_4[26]py_2N_4^{4+}$ receptor provides a large and flexible cavity to accommodate the studied anions. Molecular recognition is based in electrostatic interactions rather than in multiple hydrogen-bonding interactions acting cooperatively. By contrast, the $[Cu_2([26]py_2N_4)]^{4+}$ receptor has a well-shaped cavity with adequate size to uptake these anions as bridging ligands with formation of four Cu–O bonds. The ox^{2-} anion is encapsulated within the cascade complex while the remaining anions are located above the N_6 macrocyclic plane, suggesting a selective coordination behaviour of this receptor. In spite of our molecular simulation being carried out in gas phase, the modelling results are consistent with the solution studies.

Introduction

Anion recognition is an active area of supramolecular chemistry, stimulated by the chemical and biological importance of anions.[1–4] The design and synthesis of unusual receptors are also a challenge for researchers. Up to now various types of synthetic receptors for the binding of anions have been developed, although receptors for the selective binding of nonspherical anions are scarce.[1–6] Therefore there is a great need for novel anion receptors in order to better characterise anion association patterns and to obtain novel binding features.

Carboxylate anions play an important role in organic, environmental and biological processes. The carboxylate functions of enzymes and antibodies contribute to their specific biochemical behaviour and they are critical components of numerous metabolic processes.[5]

The binding of anionic substrates by a specific receptor results essentially from electrostatic interactions and hydrogen-bonding formation. Additional π–π stacking, van der Waals interactions or hydrophobic effects strongly contribute to the selective recognition process. Protonated polyazamacrocycles and cryptands can bind anions by electrostatic interactions, and simultaneously by hydrogen-bonding interactions between protonated nitrogen of the receptor and an acceptor atom from the substrate. These receptors are particularly interesting in the recognition of anions when they are completely charged in neutral or slightly acidic

[a] Instituto de Tecnologia Química e Biológica, UNL, Apartado 127, 2781-901 Oeiras, Portugal
Fax: +351-214-41-12-77
E-mail: delgado@itqb.unl.pt
[b] Instituto Superior Técnico, Departamento de Química, Av. Rovisco Pais, 1049-001 Lisboa, Portugal
[c] Departamento Química, CICECO, Universidade de Aveiro, 3810-193 Aveiro, Portugal

Supporting information for this article is available on the WWW under http://www.eurjic.org or from the author.

aqueous solutions. Therefore, among the various types of synthetic receptors for the recognition of anions, polyamines have an important place, especially in aqueous environments.[1–6] The binding of anions by one or more metal centres forming cascade complexes is also a rich field of research. Metal complexes as receptors covalently bind anions, and then the interactions are in general stronger than those observed when only electrostatic or hydrogen-bonding interactions exist.[7,8]

In the present work the hexaazamacrocycle, 3,10,18,25,31,32-hexaazatricyclo[25.3.1.1^{12,16}]dotriaconta-1(31),12,14,16(32),27,29-hexaene ([26]py$_2$N$_4$),[9] was used directly as a ditopic receptor in the form of tetraammonium hydrochloride salt (H$_4$[26]py$_2$N$_4$·4Cl) for the study of anion-binding properties (see Scheme 1). The dicopper(II) complex of [26]py$_2$N$_4$ was also used as a receptor in cascade associations with the same anions. These receptors allowed a systematic evaluation of the main features involved in host–guest binding interactions with dicarboxylate anions with different sizes and flexibilities, such as ox^{2-}, mal^{2-}, suc^{2-}, fu^{2-} and ma^{2-} (see Scheme 2). The association constants were determined using potentiometric methods. Additional UV/Vis and EPR spectroscopic techniques were performed for the study of the cascade dicopper complexes. In order to give further insight into the solution results, molecular modelling studies comprising molecular mechanics and dynamics simulations were undertaken in gas phase.

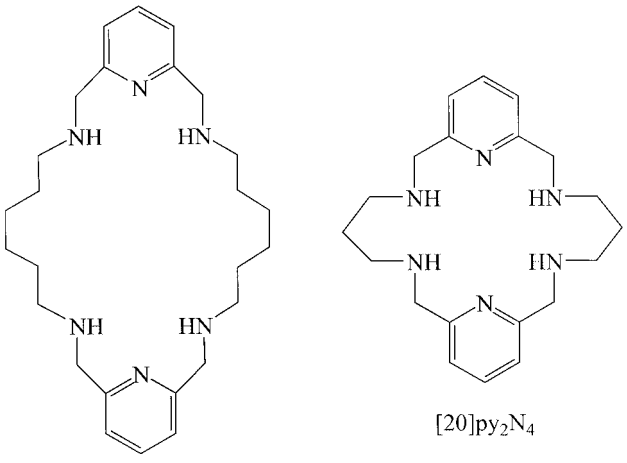

Scheme 1.

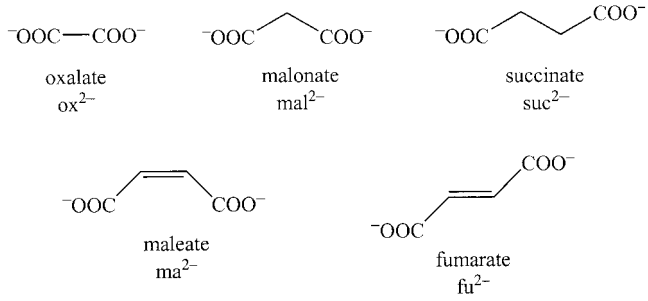

Scheme 2.

Results and Discussion

Anionic Associations with the Receptor H$_4$[26]py$_2$N$_4^{4+}$

The association constants of H$_4$[26]py$_2$N$_4^{4+}$ with ox^{2-}, mal^{2-}, suc^{2-}, fu^{2-} and ma^{2-} were determined in aqueous solutions at 298.0 K and 0.10 mol·dm^{-3} KCl, using the HYPERQUAD programme.[10] The guests are dicarboxylate anions that differ in shape, size and rigidity. The values obtained were collected in Table 1.

As the final results strongly depend on the protonation constants of the guest anions and the reported values are spread out,[11] we redetermined them in our experimental conditions and the values obtained are compiled in Table 2. The protonation constants of [26]py$_2$N$_4$ were also determined in the same experimental conditions. The values found were within the usual standard deviations for those determined before in KNO$_3$, therefore the values already published have been adopted[9] (see Table 3).

Only three constants, corresponding to the following equilibria, were found:

$$H_4[26]py_2N_4^{4+} + HA^- \rightleftharpoons \{H_5[26]py_2N_4(A)\}^{3+} \text{ (species 511)} \qquad K_1$$

$$H_4[26]py_2N_4^{4+} + A^{2-} \rightleftharpoons \{H_4[26]py_2N_4(A)\}^{2+} \text{ (species 411)} \qquad K_2$$

$$H_3[26]py_2N_4^{3+} + A^{2-} \rightleftharpoons \{H_3[26]py_2N_4(A)\}^{+} \text{ (species 311)} \qquad K_3$$

The main species corresponds to the formation of $\{H_4[26]py_2N_4(A)\}^{2+}$, which exists in solution from about 4 to 9 pH. The $\{H_5[26]py_2N_4(A)\}^{3+}$ and $\{H_3[26]py_2N_4(A)\}^{+}$ species exist in smaller percentages, the former at lower pH and the latter at higher pH values. A typical species distribution diagram is represented in Figure 1 for the case of malonate anion, using the HYSS programme.[12]

Table 1. Overall stability constants (log $\beta_{H_hL_lA_a}$)[a,b] and stepwise formation constants ($K_{H_hL_lA_a}$)[a] for the interaction of H$_4$[26]py$_2$N$_4^{4+}$ with ox^{2-}, mal^{2-}, suc^{2-}, fu^{2-} and ma^{2-}, where L denotes the [26]py$_2$N$_4$ ligand and A the anion. I = 0.10 mol·dm^{-3} in KCl at 298.0 K.

Species	ox^{2-}		mal^{2-}		suc^{2-}		fu^{2-}		ma^{2-}	
hla	log $\beta_{H_hL_lA_a}$	$K_{H_hL_lA_a}$	log $\beta_{H_hL_lA_a}$	$K_{H_hL_lA_a}$	log $\beta_{H_hL_lA_a}$	$K_{H_hL_lA_a}$	log $\beta_{H_hL_lA_a}$	$K_{H_hL_lA_a}$	log $\beta_{H_hL_lA_a}$	$K_{H_hL_lA_a}$
511	39.97(7)	91.2	41.54(5)	93.3	40.95(8)	24.0	39.91(5)	44.7	41.75(9)	50.1
411	36.53(3)	204.2	36.80(2)	380.2	36.65(1)	269.2	36.60(1)	239.9	36.55(3)	213.8
311	28.11(8)	52.5	28.57(5)	151.3	–	–	28.47(3)	120.2	28.34(5)	89.1

[a] See text for definition of the association constants. [b] Values in parentheses are standard deviations in the last significant figures.

Table 2. Protonation constants (log $\beta_{H_hA_a}$) of oxalate (ox^{2-}), malonate (mal^{2-}), succinate (suc^{2-}), maleate (ma^{2-}) and fumarate (fu^{2-}), their stability constants (log $\beta_{Cu_mH_hA_a}$) with Cu^{2+}, and the corresponding stepwise constants, log K. T = 298.0 ± 0.1 K; I = 0.10 mol·dm^{-3} in KCl.[a]

Ion	Species	ox^{2-}		mal^{2-}		suc^{2-}		ma^{2-}		fu^{2-}	
	mha	log β	log K	log β	log K	log β	log K	log β	log K	log β	log K
H^+	011	3.792(3)	3.792	5.35(1)	5.35	5.350(7)	5.350	5.826(4)	5.826	4.043(4)	4.043
	021	5.04(9)	1.25	8.04(1)	2.69	9.376(8)	4.026	7.61(2)	1.78	6.833(6)	2.790
Cu^{2+}	101	5.23(8)	5.23	4.76(2)	4.76	2.94(4)	2.93	3.45(3)	3.45	–	–
	102	8.82(5)	3.59	7.45(9)	2.69	–	–	6.02(9)	2.57	–	–

[a] Values in parenteses are standard deviations in the last significant figures. A denotes the anion.

Table 3. Protonation constants (log β_{H_hL}) of [26]py_2N_4 and its stability constants with Cu^{2+} (log $\beta_{Cu_mH_hL_l}$) and the corresponding stepwise constants, log K. T = 298.0 ± 0.1 K; I = 0.10 mol·dm^{-3} in KCl.[a]

Ion	Species *mhl*	log β	log K
H^+	011	9.18	9.18
	021	17.87	8.69
	031	26.39	8.52
	041	34.22	7.83
	051	35.73	1.51
Cu^{2+}	101	14.09	14.09
	111	22.27	8.18
	121	29.49	7.22
	131	33.02	3.53
	201	25.20	11.11
	211	29.38	4.18
	2–11	17.45	–7.75
	2–21	8.63	–8.82
	2–31	–2.64	–11.27
	2–41	–14.18	–11.54

[a] See also ref.[9]

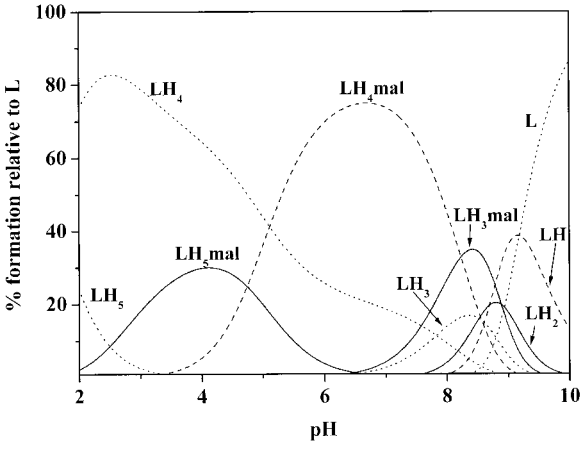

Figure 1. Species distribution curves calculated for the H_4[26]-$py_2N_4^{4+}$/mal^{2-} association in 1:1 ratio, C_L = C_{mal} = 2.00×10^{-3} mol·dm^{-3}, L being the macrocyclic ligand.

The values determined are not especially high, but the receptor is selective for malonate anion (see Figure 2). As can be observed, the K_2 values increase from oxalate to malonate and then successively decrease for the other anions, indicating that the size of the anion is the most important feature for the best association to the receptor. The overall basicity and the rigidity of the anions seem not to be very important factors for the interaction.

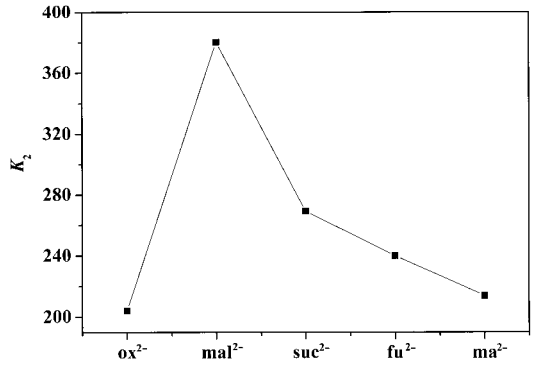

Figure 2. Plot of K_2 in function of the studied anions with different sizes and rigidities.

Cascade Dicopper Complexes

Potentiometric Measurements

The stability constants of [26]py_2N_4 with Cu^{2+} ion determined in aqueous solution at 298.0 K and 0.10 mol·dm^{-3} in KCl are also collected in Table 3.[9] For the Cu^{2+}/[26]py_2N_4 2:1 stoichiometry only dinuclear species are formed, {$[Cu_2L(H_2O)_4]^{4+}$, $[Cu_2(HL)(H_2O)_4]^{5+}$ and $[Cu_2L(H_2O)_{4-i}(OH)_i]^{4-i}$ (i = 1–4 and L = [26]py_2N_4 after pH = 4).[9] Free Cu^{2+} ions almost disappear from the solution at pH values of about 5 to yield $[Cu_2L(H_2O)_4]^{4+}$, which is the main species from pH 5 to about 8, followed by the successive hydrolysis of the four H_2O molecules directly bound to the two copper centres, $[Cu_2L(OH)_i]^{4-i}$ (i = 1–4) (see also Table 3). The X-ray single-crystal structure of the dicopper complex with a related ligand [20]py_2N_4, having propyl spacers between the pyridine heads (see Scheme 1), showed that two water molecules are directly coordinated to each copper centre,[9] and the same species was confirmed in aqueous solution.[13] Each copper centre is located at each head of the macrocycle, displaying a distorted square-pyramidal coordination environment with the basal plane defined by three consecutive nitrogen donors and one water molecule and the apical position fulfilled with the other water molecule at a longer distance than the equatorial one.[9] Therefore the presence of $[Cu_2L(H_2O)_4]^{4+}$ confirmed in our solution results led us to assume that an iden-

tical structure is adopted by the complex studied in the present work.

The predisposition of $[26]py_2N_4$ to form dinuclear complexes with copper centres, also confirmed by EPR studies,[9] led us to take advantage of this specific feature for the study of cascade complexes with dicarboxylate anions to investigate whether these guests bridge the two metal centres or, in contrast, two guests coordinate to each copper centre.

The association constants of the cascade complexes formed by addition of the anions to aqueous solutions of $[Cu_2([26]py_2N_4)(H_2O)_4]^{4+}$ at 298.0 K were determined using potentiometric measurements. The studied anions are ox^{2-}, mal^{2-}, suc^{2-} and ma^{2-} (see Scheme 2). The results are summarised in Table 4, and were obtained using the protonation constants of $[26]py_2N_4$ and of the anions and their stability constants with copper determined in our experimental conditions compiled in Table 2 and Table 3.

Several species were found in solution involving mononuclear and dinuclear complexes, mainly protonated and hydrolysed species as well as the expected complexes $[Cu_2([26]py_2N_4)(A)(H_2O)_x]^{2+}$ or $[Cu_2([26]py_2N_4)(A)_2(H_2O)_y]$, A being the guest anion, as can be seen in Table 4.

The first conclusion derived from the data of Table 4 is the distinct behaviour exhibited by oxalate and malonate substrates when compared with maleate, the succinate displaying intermediate features. Oxalate and malonate form cascade complexes with $[Cu_2([26]py_2N_4)(H_2O)_4]^{4+}$ involving only one anion, which necessarily will bridge the two copper atoms because of the symmetrical arrangement of the dinuclear complex. The two other studied anions, succinate and maleate, form species containing two anionic substrates, although species with only one suc^{2-} anion were also found. When two substrates are involved, each one can be directly coordinated to each copper, forming a dinuclear complex of independent centres, or both anions bridge the two metal centres. The adopted structure will be the result of a delicate balance of strain energies. Indeed the folded structure adopted by the dinuclear complex will rearrange for the encapsulation of the bridging anion(s), and the expended energy for the rearrangement should only be compensated by stronger interactions of the anion to the copper centres; this means anions can be better accommodated into the topology offered by the cavity formed between both copper centres.

The main species formed in the 5–9 pH range is $[Cu_2([26]py_2N_4)(A)(H_2O)_x]^{2+}$ for A = ox^{2-} or mal^{2-}, while for A = suc^{2-} this species and $[Cu_2([26]py_2N_4)(A)_2(H_2O)_x]$ overlap (and also with $[Cu_2([26]py_2N_4)(H_2O)_4]^{4+}$ when the amount of substrate is increased, such as for 2:1:2 Cu/$[26]py_2N_4$/suc^{2-} stoichiometries). For A = ma^{2-}, $[Cu_2([26]py_2N_4)(A)_2(H_2O)_y]$ is the major species, at least for the 2:1:2 ratio, although for lower substrate proportions the significance of $[Cu_2([26]py_2N_4)(H_2O)_4]^{4+}$ increases for slightly lower pH values. By potentiometric measurements, the number of water molecules in the complexes, *x* and *y*, was not possible to be determined, because in all cases the best models with coordination chemistry sense, accepted by the HYPERQUAD programme,[10] only contain species with one water molecule for which the corresponding hydrolysis constant was determined (see Table 4). For pH values lower than 5, mononuclear and dinuclear protonated complexes, involving the anion or not, are formed, and for pH values higher than 8 the water molecule of the cascade complexes starts to be hydrolysed.

However, in all cases the hydrolysed complexes $[Cu_2([26]py_2N_4)(H_2O)_{4-x}(OH)_x]^{4-x}$ replace the cascade dinuclear species containing the dicarboxylate, at high pH (>8), al-

Table 4. Overall stability constants ($\log \beta_{Cu_mH_hL_lA_a}$)[a,b] for the equilibria of $[Cu_2([26]py_2N_4)(H_2O)_4]^{4+}$ with ox^{2-}, mal^{2-}, suc^{2-} and ma^{2-}, where L is the macrocyclic ligand $[26]py_2N_4$ and A the anion. I = 0.10 mol·dm^{-3} in KCl at 298.0 K.

Species *mhla*	ox^{2-} $\log \beta_{Cu_mH_hL_lA_a}$	mal^{2-} $\log \beta_{Cu_mH_hL_lA_a}$	suc^{2-} $\log \beta_{Cu_mH_hL_lA_a}$	ma^{2-} $\log \beta_{Cu_mH_hL_lA_a}$
1411	43.94(2)	42.29(1)	41.82(4)	–
1311	39.87(7)	38.92(1)	–	–
1211	[35.0][c]	[33.5][c]	–	–
1111	31.04(9)	29.70(1)	30.52(9)	–
1011	–	23.29(4)	–	–
1–111	–	–	13.29(5)	
2011	30.17(1)	29.13(1)	28.78(7)	–
2111	35.49(6)	34.34(2)	33.41(9)	–
2211	39.78(5)	–	–	–
2–111	21.07(2)	20.44(2)	–	–
1412	–	–	–	47.52(2)
1312	–	–	–	43.47(4)
1212	–	–	–	39.35(4)
1112	–	–	–	34.56(3)
1012	–	–	–	26.64(7)
2012	–	–	32.07(5)	32.59(3)
2112	–	–	36.98(9)	–
2–112	–	–	23.23(6)	23.39(8)

[a] See Experimental, Calculation of Stability Constants, for definitions. [b] Values in parenthesis are standard deviations in the last significant figures. [c] Values in brackets are determined with large standard deviations; because the species exist in solution in small amounts (<10%), the final model was refined without these species.

though, depending on A, small amounts of mononuclear species, $\{Cu([26]py_2N_4)A\}$ or $\{Cu([26]py_2N_4)A_2\}^{2-}$, were also found. This indicates that the dicarboxylate anions, whether bridging the two copper centres or not, are replaced by OH^- groups at high pH values, or in other words, the cascade complexes dissociate, yielding successively the species $[Cu_2([26]py_2N_4)(H_2O)_{4-x}(OH)_x]^{4-x}$ with an increase of pH.

These and other features of the behaviour of these complexes in aqueous solutions as a function of the pH can be observed in Figure 3 and Figure 4 for mal^{2-} and suc^{2-} anions, respectively. The comparison of the species distribution diagrams for suc^{2-} and ma^{2-} anions (see the diagram for ma^{2-} in the Supporting Information) emphasises the intermediate behaviour of the succinate anions, as already mentioned. Indeed between pH 5 and 9 both species, $[Cu_2([26]py_2N_4)(suc)(H_2O)_x]^{2+}$ and $[Cu_2([26]py_2N_4)(suc)_2(H_2O)_x]$, exist in solution in percentages depending on the suc^{2-} ratio, while only the $[Cu_2([26]py_2N_4)(ma)_2(H_2O)_x]$ complex is formed in the same pH range (for lower anion ratios the percentage of $[Cu_2([26]py_2N_4)(H_2O)_4]^{4+}$ increases in both cases).

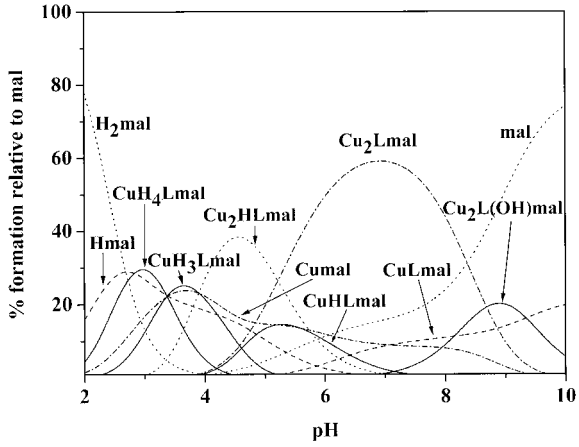

Figure 3. Species distribution curves calculated for the system $[Cu_2([26]py_2N_4)(H_2O)_x]^{4+}/mal^{2-}$ for 1:1 ratio, $C_{complex} = C_{mal} = 2.00 \times 10^{-3}$ mol·dm^{-3}, "complex" being the dicopper complex, L the $[26]py_2N_4$ and mal^{2-} the malonate anion guest.

The copper–substrate interaction, measured by the magnitude of the association constant corresponding to the equilibrium $[Cu_2([26]py_2N_4)(H_2O)_4]^{4+} + A^{2-} \rightleftharpoons [Cu_2([26]py_2N_4)(A)(H_2O)_x]^{2+}$ (Table 4 and Table 5) is stronger for A = ox^{2-}, followed by mal^{2-} and then suc^{2-}, the values being 4.97, 3.93 and 3.58 log units, respectively (see Table 5, where the stepwise constants and the corresponding equilibrium reactions are summarised). On the other hand, the corresponding constant for the equilibrium $[Cu_2([26]py_2N_4)(H_2O)_4]^{4+} + 2\ A^{2-} \rightleftharpoons [Cu_2([26]py_2N_4)(A)_2(H_2O)_x]$ is higher for ma^{2-} anions, being 7.39 for this anion and 6.87 for suc^{2-}, in log units. Then the strength of the Cu···A···Cu interaction decreases with the increase of the length of the spacer between the two carboxylate sites, being stronger for oxalate and weaker for succinate anions. This trend is opposite to the overall basicity of the anions, which follows the order succinate > malonate >> oxalate (see Table 2). The same happens with the species involving two carboxylate anions, suggesting that the size of the anion and its rigidity are the most important factors for the verified order of association constants.

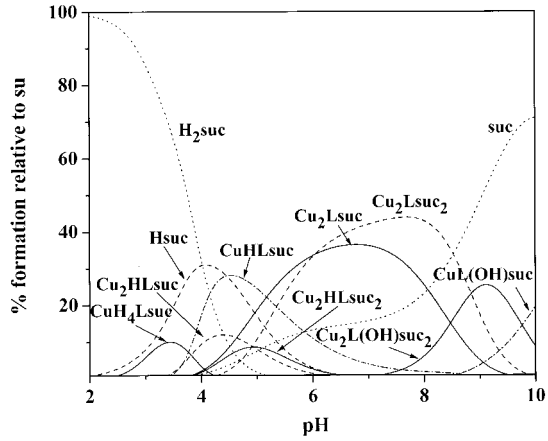

Figure 4. Species distribution curves calculated for the system $[Cu_2([26]py_2N_4)(H_2O)_x]^{4+}/suc^{2-}$ for 1:1 ratio, $C_{complex} = C_{suc} = 2.00 \times 10^{-3}$ mol·dm^{-3}, "complex" being the dicopper complex and suc^{2-} the guest succinate anion.

Table 5. Stepwise association constants (log *K*) corresponding to the indicated equilibrium calculated from the values of Table 4.

Equilibrium	ox^{2-}	mal^{2-}	suc^{2-}	ma^{2-}
$CuH_4L + A \rightleftharpoons CuH_4LA$	7.13	3.92	3.45	–
$CuH_3L + A \rightleftharpoons CuH_2LA$	6.85	5.90	–	–
$CuHL + A \rightleftharpoons CuHLA$	8.77	7.43	8.25	–
$CuL + A \rightleftharpoons CuLA$	–	9.2	–	–
$Cu_2H_2L + A \rightleftharpoons Cu_2H_2LA$	6.61	–	–	–
$Cu_2HL + A \rightleftharpoons Cu_2HLA$	6.11	4.96	4.63	–
$Cu_2L + A \rightleftharpoons Cu_2LA$	4.97	3.93	3.58	–
$Cu_2(H_{-1}L) + A \rightleftharpoons Cu_2(H_{-1}L)A$	3.62	2.99	–	–
$CuH_4L + 2\ A \rightleftharpoons CuH_4LA_2$	–	–	–	7.67
$CuH_3L + 2\ A \rightleftharpoons CuH_3LA_2$	–	–	–	10.45
$CuH_2L + 2\ A \rightleftharpoons CuH_2LA_2$	–	–	–	9.86
$CuHL + 2\ A \rightleftharpoons CuHLA_2$	–	–	7.60	12.29
$CuL + 2\ A \rightleftharpoons CuLA_2$	–	–	–	12.55
$Cu_2L + 2\ A \rightleftharpoons Cu_2LA_2$	–	–	6.87	7.39
$Cu_2(H_{-1}L) + 2\ A \rightleftharpoons Cu_2(H_{-1}L)A_2$	–	–	5.78	5.94

Spectroscopic Measurements

The UV/Vis spectrum of aqueous $[Cu_2([26]py_2N_4)(H_2O)_4]^{4+}$ solution was recorded at pH ≈ 6. The complex exhibits a broad d-d band at 660 nm and three main bands in the UV region at 288, 262 and 206 nm (see Table 6). The intense band at 262 nm was attributed to ligand-to-metal charge transfer absorption (LMCT). The addition of increasing amounts of the studied anion guests led to a hypochromism (a decrease in the molar absorptivity) and to a shift in wavelength of the visible band in all cases, the shifts being smaller in the UV region (see Table 6). However, while the shift of the visible band is to the red in the presence of ox^{2-}, a blue shift is observed for the other three anions, although very small for mal^{2-}.

Table 6. Spectroscopic UV/Vis data for $[Cu_2([26]py_2N_4)(H_2O)_4]^{4+}$ and upon addition of dicarboxylate anions.

Complex	pH	UV/Vis λ_{max}/nm (ε_{molar}/dm^3·mol^{-1}·cm^{-1})
$[Cu_2([26]py_2N_4)(H_2O)_4]^{4+}$	5.76	206 (sh., 19744.1); 246 (sh., 9707.5); 262 (16352.8); 266 (sh., 14140.8); 288 (5978.1); 660 (351.0)
$[Cu_2([26]py_2N_4)(H_2O)_4]^{4+}$ + ox^{2-}	7.54	200 (sh., 33290.7); 206 (sh., 30466.2); 248 (sh., 12285.2); 260 (17404.0); 266 (sh., 15128.0); 282 (sh., 6517.4); 674 (341.3); 820 (sh., 138.9)
$[Cu_2([26]py_2N_4)(H_2O)_4]^{4+}$ + mal^{2-}	7.10	204 (sh., 19323.6); 244 (sh., 10804.4); 260 (15493.6); 266 (sh., 13025.6); 280 (5402.2); 658 (338.2); 820 (sh., 55)
$[Cu_2([26]py_2N_4)(H_2O)_4]^{4+}$ + suc^{2-}	7.16	204 (sh., 19890.3); 246 (sh., 12669.1); 260 (16855.6); 266 (sh., 14012.8); 280 (5968.9); 650 (296.2)
$[Cu_2([26]py_2N_4)(H_2O)_4]^{4+}$ + ma^{2-}	7.72	202 (38592.3); 208 (sh., 33418.6); 250 (sh., 16517.4); 258 (18446.1); 266 (sh., 15511.9); 282 (6663.6); 650 (336.4)

The red shift of the visible band observed when the substrate is ox^{2-} assigns the presence of this anion, but also reveals a change of the structure adopted by the copper centres in this complex because of the bridging anion,[14–17] while the blue shifts resulting from the presence of the other dicarboxylates should be a consequence of the stronger equatorial field derived from the replacement of a water molecule by the oxygen atom of the carboxylate group of the anion.

The X-band EPR spectrum of a frozen water/DMSO (1:1 v/v) solution of $[Cu_2([26]py_2N_4)(H_2O)_4]^{4+}$ is typical of a coupled dinuclear copper triplet-state centre with a $S = 1$ state and zero-field splitting, having two types of signals in the $\Delta M_s = 1$ and $\Delta M_s = 2$ regions[9,18,19] (see Figure 5). The $\Delta M_s = 2$ transition signal reveals a spin-exchange interaction between the two copper atoms, but the signal is very small and the seven hyperfine lines resulting from the coupling of each unpaired electron with the two copper nuclei cannot be observed.

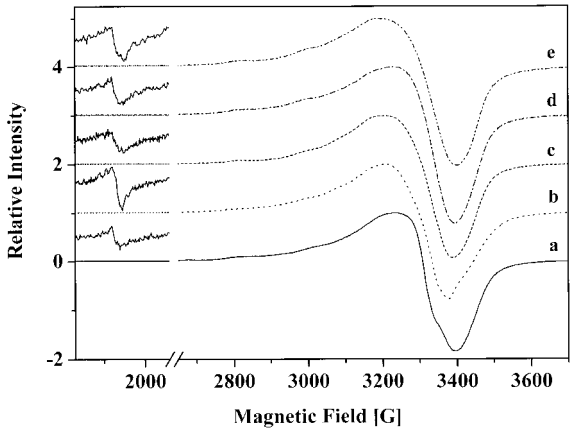

Figure 5. EPR X-band spectra of $[Cu_2([26]py_2N_4)(H_2O)_4]^{4+}$ (bottom) at 6.4 K and of $[Cu_2([26]py_2N_4)(A)(H_2O)_x]^{2+}$, A being successively ox^{2-} (at 11.4 K), mal^{2-} (at 11.4 K), suc^{2-} (at 6.4 K) and ma^{2-} (at 6.4 K). The signal at low field for each complex was amplified and placed above the axis. All the complexes were prepared at 2.0×10^{-3} mol·dm^{-3} in DMSO/H_2O (1:1). The spectra were recorded at the microwave power of 2.4 mW, modulation amplitude of 1.0 mT and at the frequency (ν) 9.646 GHz.

When oxalate anion is added to the solution of the dinuclear copper complex, a new signal at ≈3500 G appears, and in the $\Delta M_s = 2$ region the hyperfine structure is now perceptible, revealing a shorter distance between both copper centres because of the presence of the bridging anion. Indeed for $\Delta M_s = 1$ transitions, two groups of peaks spaced on either side of $g \approx 2$ emerge, showing an overall width as a function of r (the distance between the two copper centres).[20] Considering D, the zero-field splitting within the triplet state, built up from a dipolar contribution D_{dip}, and an exchange contribution, D_{ex}: $D = D_{ex} + D_{dip}$, and if we consider $D_{ex} \approx 0$ (valid for $-J \leq 30$ cm^{-1}), the r distance can be evaluated directly from D.[21] It was possible to estimate the D value from the spectrum only for the case of $[Cu_2([26]py_2N_4)ox]^{2+}$. The spectra of the cascade complexes for the other anions are too broad to allow the determination of the D value (see Figure 5). However for $[Cu_2([26]py_2N_4)ox]^{2+}$ the $2D$ value was calculated by the difference between the Hz_2 and Hz_1 transitions, yielding to 0.0128 cm^{-1}. Even in this case it was difficult to observe all the lines of the two expected septets, however from the more intense lines (third to fifth) it was possible to obtain a satisfactorily accurate value of the zero-field splitting constant. Taking $g_{\|} = 2.237$ and $g_{\perp} = 2.10$, obtained directly from the spectrum, the value of 6.3 ± 0.2 Å was determined for the copper–copper distance in the $[Cu_2([26]py_2N_4)ox]^{2+}$ complex.

Molecular Modelling

In order to give a further insight in our solution studies, the binding ability of $[26]py_2N_4$ to accommodate ox^{2-}, mal^{2-}, suc^{2-} and ma^{2-} anions in its tetraprotonated form or, alternatively, as bridging ligands in its copper dinuclear complex was evaluated in gas phase through molecular mechanics (MM) and molecular dynamics (MD) simulations using the Universal Force Field[22] within the Cerius2 software package.[23]

The molecular modelling studies started with the conformational analysis of the $H_4[26]py_2N_4^{4+}$ following quenching dynamics methods over 2 ns. 10000 conformations were generated and subsequently minimised by MM as described in the experimental section. The final structures have energies in a wide range of 667.43–716.94 kcal·mol^{-1}. In spite of the presence of the two pyridine heads in the macrocyclic framework, between these two limits, the energy changes almost continuously. This result is expected due to the large

number of single bonds with corresponding endocyclic torsion angles determining a geometric arrangement between a *gauche* and a *trans* configuration. The two pyridine rings oscillate continuously, with the dihedral angle between them ranging from 0.1° to 134.3°. Furthermore, the intermolecular distance between the pyridine nitrogen donors, ranging from 7.591 to 11.261 Å, indicates that the receptor can adopt conformational shapes with different cavity sizes. The interactions between this receptor and ox^{2-}, mal^{2-}, suc^{2-} and ma^{2-} were further investigated, docking each one of these four anions to the lowest energy conformation of $H_4[26]py_2N_4^{4+}$, also using a MD quenching methodology. The lowest energy structures found, presented in Figure 6, show that the $H_4[26]py_2N_4^{4+}$ receptor adopts different conformational shapes providing a suitable cavity to encapsulate all four of these dicarboxylate anions. The electrostatic bonding interactions dictate the molecular recognition between the receptor and each anion in gas phase. Indeed the binding energy determined from the difference between the energy of the inclusion compound and the sum of the individual energies of the $H_4[26]py_2N_4^{4+}$ receptor (lowest energy conformation) and the anion, listed in Table 7, indicates that in all cases the inclusion process is highly favourable, the electrostatic term being the largest contributor. Further, the dynamic behaviour of each inclusion compound was evaluated by MD at 300 K over 1 ns. In Table 8 the most significant short N–H···O hydrogen contacts found during the simulations using a cut-off of 2.5 Å for H···O distances are listed. The number of hydrogen-bonding interactions increases with the size of the anion following the order ox^{2-}, ma^{2-}, mal^{2-} and suc^{2-}. The ox^{2-} anion establishes with the $H_4[26]py_2N_4^{4+}$ receptor only one N–H···O hydrogen bond during about 170 ps of simulation with a Φ frequency of only 3.2 s^{-1}, while the oxygen atoms of the two carboxylate groups of ma^{2-} are involved in two hydrogen bonds with two N–H binding sites for almost the entire duration of the simulation. However, these contacts have low frequencies of 2.7 and 3.1 ps^{-1}, occurring separately for almost the whole time. The mal^{2-} and suc^{2-} form through two oxygen atoms, respectively, four and five N–H···O hydrogen bonds with the $H_4[26]py_2N_4^{4+}$ receptor. Again in both cases all these intermolecular contacts show low frequencies and only occasionally (without statistical significance) act cooperatively for the molecular recognition phenomena. These results show that the $H_4[26]py_2N_4^{4+}$ receptor has high flexibility and a too large cavity that is inappropriate for molecular recognition of the anions.

Table 7. Binding energy for $\{(H_4[26]py_2N_4)(A)\}^{2+}$ supramolecular compounds in gas phase.

	Energy/kcal·mol^{-1}			
	Total energy	Electrostatic energy	ΔE_{total}[a]	$\Delta E_{electrostatic}$[b]
$\{(H_4[26]py_2N_4)(ox)\}^{2+}$	424.05	351.75	–495.56	–490.37
$\{(H_4[26]py_2N_4)(mal)\}^{2+}$	285.48	223.16	–492.94	–479.71
$\{(H_4[26]py_2N_4)(suc)\}^{2+}$	272.98	212.06	–474.35	–460.96
$\{(H_4[26]py_2N_4)(ma)\}^{2+}$	334.81	261.78	–481.24	–468.86
ox^{2-}	240.63	234.22	–	–
mal^{2-}	99.43	94.96	–	–
suc^{2-}	68.35	65.12	–	–
ma^{2-}	137.07	122.73	–	–
$H_4[26]py_2N_4^{4+}$	678.98	607.90	–	–

[a] $\Delta E_{total} = E_{t(supramolecule)} - E_{t(anion)} - E_{t(receptor)}$. [b] $\Delta E_{electrostatic} = E_{e(supramolecule)} - E_{e(anion)} - E_{e(receptor)}$.

The length of the bridge between the two copper centres supported by the $[Cu_2([26]py_2N_4)]^{4+}$ complex can be established ascertaining the Cu···Cu distances allowed by the macrocycle without any additional steric strain from the presence of other ligands in the metal co-ordination spheres. On the other hand, when two copper centres are

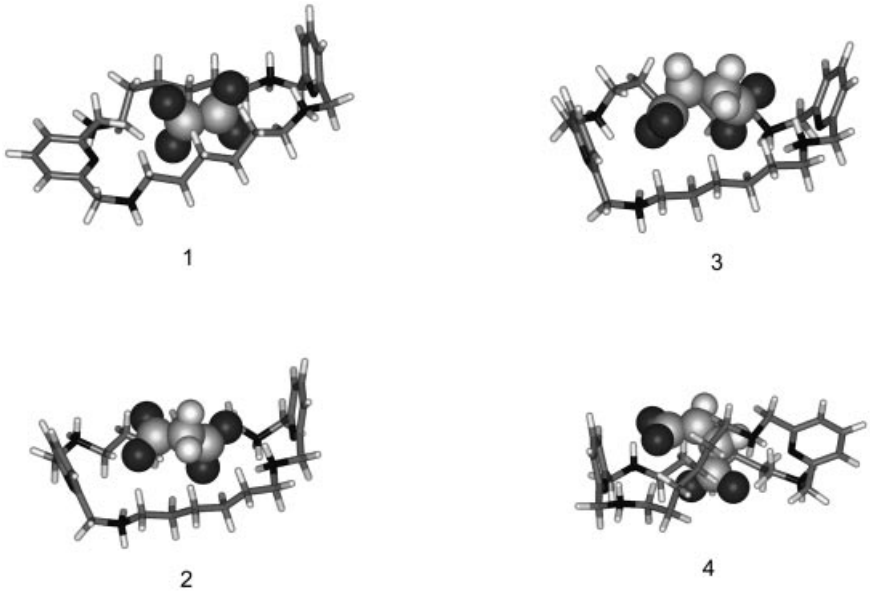

Figure 6. Lowest energy structures found for $\{(H_4[26]py_2N_4)(A)\}^{2+}$ supramolecular compounds, with A equal to ox^{2-} (1), mal^{2-} (2), suc^{2-} (3) and ma^{2-} (4).

Table 8. Hydrogen-bonding interactions found for $\{(H_4[26]py_2N_4)(ox)\}^{2+}$ supramolecular compounds during the molecular dynamics simulations.

Anion	Period of simulation/ps	Φ/s^{-1}[a]	Hydrogen-bonding interactions[b]
ox^{2-}	828.3–999.8	3.2	N_1–H_a···O_1
mal^{2-}	0.8–704.1	0.71	N_1–H_b···O_1
	0.3–779.4	1.14	N_1–H_a···O_1
	1.5–905.7	0.96	N_1–H_a···O_2
	20.3–706.5	0.55	N_2–H_a···O_2
suc^{2-}	8.4–996.0	0.28	N_1–H_a···O_1
	421.4–650.7	1.33	N_1–H_b···O_1
	0.1–408.3	0.52	N_2–H_a···O_1
	5.9–642.5	0.48	N_3–H_a···O_3
	364.1–792.9	1.06	N_4–H_a···O_3
ma^{2-}	0.1–999.8	2.72	N_1–H_a···O_1
	0.3–999.6	1.20	N_3–H_a···O_3

[a] Φ is given by the ratio between the number of times and the period of simulation in which a short contact is observed. For each anion, the N–H-binding groups are labelled in a clockwise manner. [b] The oxygen donor atoms of the anions are labelled using the following atomic notation scheme: O_1 and O_2 for the first carboxylate group and O_3 and O_4 for the second one.

coordinated to $[26]py_2N_4$, the relative positions of the N–H groups, below (–) and above (+) the N_6 macrocyclic plane determine five independent conformations: + + + +, + + – –, + + + –, – + – + and + – – +. All these arrangements have to be considered in a complete analysis of the structural preferences of the coordinated macrocycle, which was undertaken following an identical MD methodology to that described for the $H_4[26]py_2N_4^{4+}$ receptor. For each $[Cu_2([26]py_2N_4)]^{4+}$ conformation a short MD simulation of 100 ps was carried out. The lowest energy conformations found are shown in Figure 7, while their corresponding energies are given in Table 9 together with the Cu···Cu distance and the dihedral angle between the two pyridine rings (called the α angle here). The energies range only between 452.0 and 464.7 kcal·mol^{-1} for + + + + and – + – + conformations, respectively. The + + – – conformation has an energy only 0.9 kcal·mol^{-1} higher than the lowest one. The electrostatic energy term is again the largest contributor for the total energy. The + + + + conformation adopts a cleft topology with an α angle of 59.5° while in the + + – – conformation the two pyridine rings are in antiperiplanar arrangement with an α angle of 164.4°. The remaining three conformations adopt an almost planar shape with the α angle ranging from 151.9° for + – – + to 173.2° for + + + –. The Cu···Cu distance is in a wide range of values between 7.790 and 8.768 Å, so it is not possible to establish any straight relationship between the separation of the two copper centres and the shape or conformation adopted. The first + + + + conformation having an almost planar shape appears at 464.3 kcal·mol^{-1} with an α angle of 160.2° and a Cu···Cu distance of 7.857 Å.

Table 9. Lowest energy conformations for the $[Cu_2([26]py_2N_4)]^{4+}$ receptor.

Conformation	Energy/kcal·mol^{-1}	Cu···Cu/Å	α/°[a]
+ + + +	452.0	8.768	59.5
+ + – –	452.9	8.814	164.4
+ + + –	457.6	8.225	173.2
+ – – +	462.1	7.750	151.9
– + – +	464.7	7.790	163.7

[a] α angle definition is given in the text.

The 3D scatter plot of the α dihedral angle versus steric energy and the Cu···Cu distance found for the conformational analysis of $[Cu_2([26]py_2N_4)]^{4+}$ in the + + + + conformation is presented in Figure 8. This plot shows that most of the conformations have a cleft shape, with the Cu···Cu distance in a narrow range from 8.9 to 9.0 Å. By contrast, the few conformations with almost planar or antiparallel arrangements accommodate a wide range of distances between 8.1 and 9.0 Å.

Alternatively, the distance between the two copper centres tolerated by the macrocyclic cavity can be ascertained from the energy profile for $[Cu_2([26]py_2N_4)]^{4+}$, calculated using our published method.[24] Here, the Cu···Cu dis-

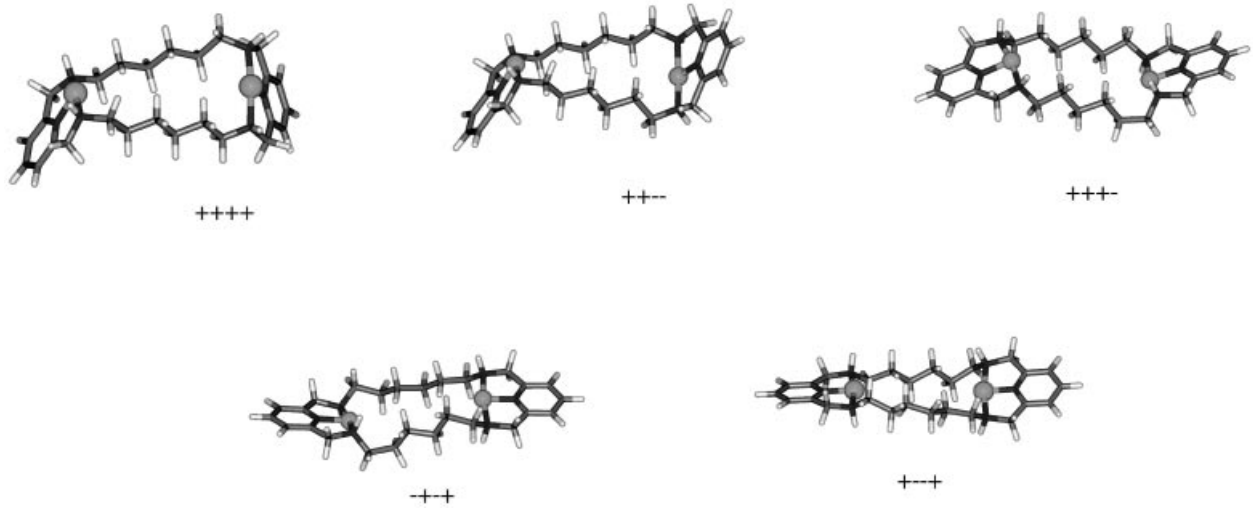

Figure 7. Lowest energy conformations for $[Cu_2([26]py_2N_4)]^{4+}$ receptor.

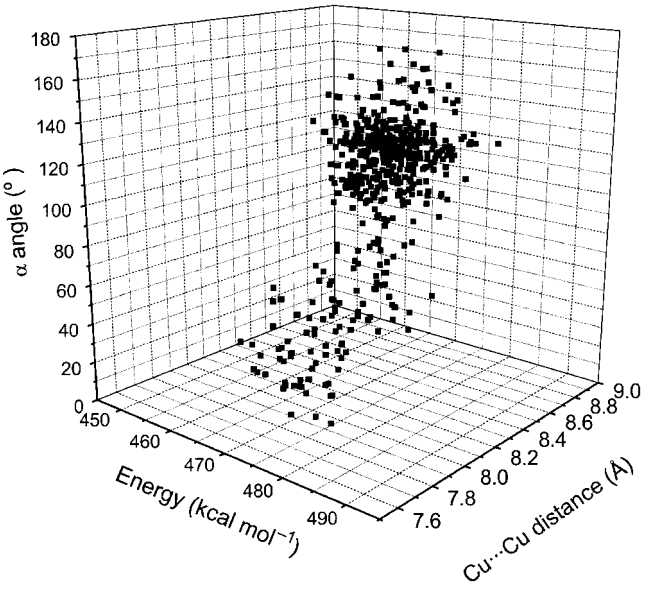

Figure 8. 3D scatter plot of the α angle against steric energy and Cu···Cu distance for $[Cu_2([26]py_2N_4)]^{4+}$ receptor.

tance was varied at 0.1 Å intervals between the limits 7.2–10.0 Å. At each distance the macrocyclic energy is minimised by MM and the resulting energies found for the + + + + cleft conformation (see Table 9), shown in Figure 9, represent the steric strain in the macrocycle caused by a specific Cu···Cu distance. The plot of Figure 9 (bottom) shows an almost deep energy profile with a minimum at 8.75 Å. When this calculation was repeated without charges (Figure 9, top), the energy profile is broad, with the macrocyclic cavity having a better tolerance for short Cu···Cu distances. This result is expected, given that the main repulsive electrostatic interaction derived from the presence of the two Cu^{2+} centres was eliminated. However, the centre of the broad minimum was only shifted 0.25 Å for shorter distances. This result suggests that the macrocycle must adopt a different conformational shape in order to accommodate bridging anions requiring shorter Cu···Cu distances, typically below 8.0 Å.

Having evaluated the steric requirements of the $[Cu_2([26]py_2N_4)]^{4+}$ complex, the interaction between this receptor (+ + + + conformation) and the ox^{2-}, mal^{2-}, suc^{2-} and ma^{2-} anions was investigated through the MD quenching technique for 100 ps. No bonds between the oxygen donors and the two copper centres were included and consequently the host–guest interactions are purely electrostatic. In Figure 10 the lowest energy arrangements found for the four cascade complexes are shown. The sum of MM energies found for isolated anions and $[Cu_2([26]py_2N_4)]^{4+}$ (lowest energy conformation) largely exceed the energy of the corresponding cascade complex, which indicates that in gas phase its formation is highly favourable in all four cases. This binding energy takes the values of –784.4, –755.6, –747.1 and –732.4 kcal·mol^{-1} for ox^{2-}, mal^{2-}, suc^{2-} and ma^{2-}, respectively. The dicarboxylate anions bridge the two copper centres through all four oxygen donors, with Cu–O

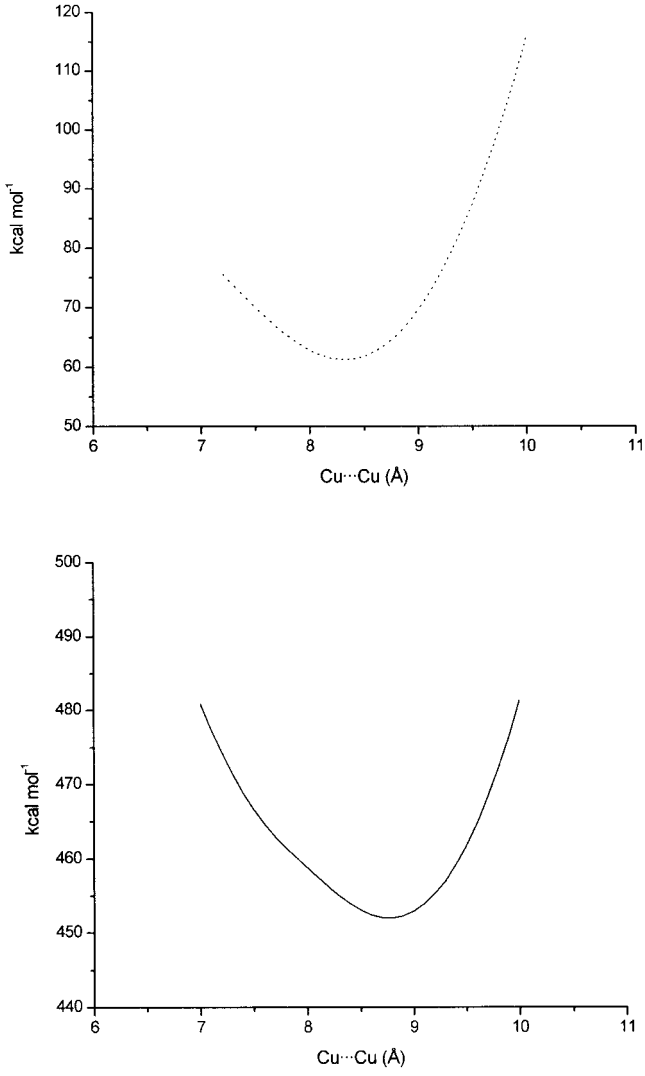

Figure 9. Plot of steric energy profile against Cu···Cu distance for $[Cu_2([26]py_2N_4)]^{4+}$ receptor with charges (solid line) and without charges (dotted line).

distances taking normal values for this type of bond, typically about 2.0 Å. However, the smaller anion ox^{2-} is inside the macrocyclic cavity, while the remaining three anions are located above the plane determined by the six nitrogen donors of the receptor. The pyridine rings are almost in a planar arrangement, making a dihedral angle of 16.3, 33.2 and 9.7° for ox^{2-}, mal^{2-} and suc^{2-}, respectively; while for ma^{2-} these rings are twisted, giving an angle of 128.1°.

Subsequently the cascade complexes were submitted to MD runs of 1 ns at room temperature. The average distances from the copper to oxygen atoms of the anions together with their small standard deviations, listed in Table 10, clearly indicate that each bridged anion remains coordinated by all four Cu–O bonds for the entire period of the simulation. In addition, the Cu···Cu distances are largely dependent on the size and the steric requirements of the bridge. Indeed the Cu···Cu distance of the lowest energy conformation of 8.768 Å was substantially shortened to 6.44(6) Å when the smallest ox^{2-} anion was included, while

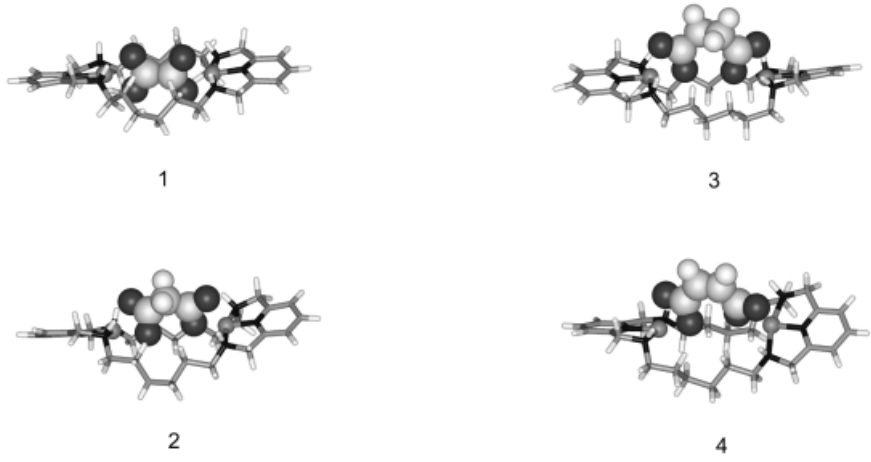

Figure 10. Lowest energy structures found for $[Cu_2([26]py_2N_4)(A)]^{2+}$ cascade complexes, with A equal to ox^{2-} (1), mal^{2-} (2), suc^{2-} (3) and ma^{2-} (4).

the ma^{2-} anion having a *cis* double bond between the two carboxylate groups kept the two metal centres at a longer distance of 6.88(15) Å. The distances between the copper centres supported by mal^{2-} and suc^{2-} bridges are 6.58(10) and 6.62(14) Å, respectively. These values are shorter than the average Cu···Cu distances for $[Cu_2([26]py_2N_4)]^{4+}$ in + + + + cleft [8.73(14) Å] and roughly planar [8.64(18) Å] topologies found from two MD simulations carried out at 300 K over 1 ns.

Table 10. Cu–O and Cu···Cu distances [Å] found for $[Cu_2([26]py_2N_4)(A)]^{2+}$ cascade complexes from MD at 300 K (A = ox^{2-}, mal^{2-}, suc^{2-} and ma^{2-}).

	ox^{2-}	mal^{2-}	suc^{2-}	ma^{2-}
Cu–O	2.045(43)	2.094(51)	2.106(54)	2.067(47)
	2.061(46)	2.082(50)	2.046(44)	2.074(48)
	2.045(43)	2.084(50)	2.058(45)	2.073(48)
	2.062(46)	2.096(51)	2.083(50)	2.067(47)
Cu···Cu	6.44(6)	6.58(10)	6.62(14)	6.88(15)

Certainly other binding scenarios between the receptor and the substrates are possible, for instance the docking of the anions from the opposite side of the N–H groups of the macrocycle. However the evaluation of all of them would be a huge task. On the other hand, the presence of other ligands leading to five- or six-coordination geometries to the copper centres were not taken into account in our calculations. In spite of these modelling studies being carried out in the gas phase, neglecting important solution effects, they show that the selective binding of ox^{2-}, mal^{2-}, suc^{2-} and ma^{2-} to the $[Cu_2([26]py_2N_4)]^{4+}$ receptor occurs. In other words, in contrast to the $H_4([26]py_2N_4)^{4+}$ receptor, in the dinuclear copper complex the macrocycle has a preorganised cavity with the two copper centres located at apparent flexible positions able to promote the uptake of these anions.

Conclusions

The macrocycle $[26]py_2N_4$ has been used as a receptor, in its tetraprotonated form or as a dicopper complex, for the recognition of dicarboxylate anions. Our solution studies revealed that the tetraprotonated form, $H_4[26]py_2N_4^{4+}$, is a weak receptor for the studied anions when compared with others,[25–30] although it is more selective for malonate. On the other hand, the dicopper complex of $[26]py_2N_4$ forms cascade complexes with oxalate and malonate with strong association constants,[31–34] the association with the bridging anion being stronger for oxalate. Additionally, the $[Cu_2([26]py_2N_4)(H_2O)_4]^{4+}$ complex can act as an optical sensor to detect and quantitatively measure oxalate spectrophotometrically by the red shift of the maximum of the visible band observed by addition of oxalate to an aqueous solution of the dinuclear copper complex. However the selectivity for oxalate is not sufficiently high for the selective detection of this anion in the presence of malonate.

Molecular mechanics and dynamics simulations were carried out in gas phase, ignoring the solvent effects. However, in spite of this limitation, our modelling studies support entirely the experimental results, showing that the cavity of $H_4[26]py_2N_4^{4+}$ is too large and too flexible for the selective binding of the studied anions. By contrast, in the $[Cu_2([26]py_2N_4)]^{4+}$ receptor the two copper centres define a well-shaped cavity suitable for the selective encapsulation of the small dicarboxylate anion, ox^{2-}. Larger dicarboxylate anions such as mal^{2-}, suc^{2-} and ma^{2-} also bridge the two copper centres, but they are located above the N_6 macrocyclic plane. Of course the receptor can interact with the oxygen donor atoms from the anions in a different way, leading to cascade complexes with R/S ratios other than 1:1. Other possible binding modes are: two bridging anions between the copper centres of the receptor or two anions axially coordinated to each copper centre. Alternatively, two $[Cu_2([26]py_2N_4)]^{4+}$ complexes are eventually linked by two anion bridges leading to the formation of dimeric or

polymeric species. However the evaluation of all binding modes even by molecular mechanics calculations is a huge task and is beyond the aims of these preliminary modelling studies.

Experimental Section

Potentiometric Measurements

Reagents and Solutions: All the chemicals were of reagent grade and used as supplied without further purification. The receptor $[26]py_2N_4$ and its tetraprotonated salt, $H_4[26]py_2N_4{\cdot}4Cl$, were prepared and characterised as reported.[9] Dicarboxylate anion solutions were prepared at about 5.00×10^{-2} mol·dm^{-3} to 2.00×10^{-3} mol·dm^{-3} from the corresponding dicarboxylic acids (analytical grade purchased to Merck) and the concentrations were checked by titration with standard 0.100 mol·dm^{-3} KOH solutions, except for fumarate, for which the disodium salt from Aldrich was used. Solutions of $Cu(NO_3)_2$ were prepared at about 0.025 mol·dm^{-3} (analytical grade) and the exact concentration checked by titration with K_2H_2edta following standard methods.[35] All the solutions were prepared using demineralised water (obtained by a Millipore/Milli-Q system). Carbonate-free solutions of the KOH titrant were obtained and maintained as described,[9] and they were discarded when the percentage of carbonate was about 0.5% of the total amount of base.

Equipment and Work Conditions: The equipment used has been described previously.[9] The temperature was kept at 298.0 ± 0.1 K; atmospheric CO_2 was excluded from the cell during the titration by passing purified nitrogen across the top of the solution in the reaction cell. The ionic strength was kept at 0.10 mol·dm^{-3} with KCl.

Measurements: The $[H^+]$ of the solutions was determined by the measurement of the electromotive force of the cell, $E = E'° + Q{\cdot}\log[H^+] + E_j$. $E'°$, Q, E_j and $K_w = ([H^+][OH])$ were obtained as described previously.[9] The term pH is defined as $-\log[H^+]$. The value of K_w was found to be equal to $10^{-13.80}$ mol^2·dm^{-6}.

The potentiometric equilibrium measurements were carried out using 25.00 cm^3 of about 2.00×10^{-3} mol·dm^{-3} $[26]py_2N_4$ solutions diluted to a final volume of 30.00 cm^3, in the absence of dicarboxylate anions and of copper(II) salt, then in the presence of each anion at 1:1 and 2:1 C_L/C_A ratios, and finally in the simultaneous presence of copper(II) and each anion at 2:1:1 and 2:1:2 $C_{Cu}/C_L/C_A$ stoichiometries. A minimum of two replicate measurements were performed. All the anions were also independently titrated alone and in the presence of copper(II) ion in the conditions described above, at 1:1 and 1:2 C_{Cu}/C_A ratios.

Calculation of Equilibrium Constants: Overall protonation constants, β_i^H, were calculated by fitting the potentiometric data obtained for all the performed titrations with the HYPERQUAD programme.[10] The protonation constants of $[26]py_2N_4$ and its stability constants with the Cu^{2+} ion had been determined before in 0.10 mol·dm^{-3} KNO_3[9] and redetermined in the present work in 0.10 mol·dm^{-3} KCl. The protonation constants of the dicarboxylic acids (oxalic, malonic, succinic, fumaric and maleic acids) and their stability constants with Cu^{2+} ion were also determined from the experimental data in the same experimental conditions, also using the HYPERQUAD programme. All these constants were taken as fixed values to obtain the equilibrium constants of the new species from the experimental data corresponding to all the titrations in different Cu/L/A or L/A stoichiometries, also using the HYPERQUAD programme. The initial computations were obtained in the form of overall stability constants, $\beta_{Cu_mH_hL_lA_a}$ or $\beta_{H_hL_lA_a}$ values, $\beta_{Cu_mH_hL_lA_a} = [Cu_mH_hL_lA_a]/([Cu]^m\times[H]^h\times[L]^l\times[A]^a)$ or $\beta_{H_hL_lA_a} = [H_hL_lA_a]/([H]^h\times[L]^l\times[A]^a)$. Cascade mononuclear species CuLA, CuH_iLA (i = 1–4), $CuLH_{-1}A$, $CuLA_2$, CuH_iLA_2 (i = 1–4), and also dinuclear species Cu_2LA, Cu_2H_iLA (i = 1–2), $Cu_2LH_{-1}A$, Cu_2LA_2, Cu_2HLA_2 and $Cu_2LH_{-1}A_2$ were found [$\beta_{CuLH_{-1}A} = \beta_{CuL(OH)A}\times K_w$, $\beta_{Cu_2LH_{-1}A} = \beta_{Cu_2L(OH)A}\times K_w$ and $\beta_{Cu_2LH_{-1}A_2} = \beta_{Cu_2L(OH)A_2}\times K_w$]. The species considered in a particular model were those that could be justified by the principles of coordination and supramolecular chemistry. The errors quoted are the standard deviations of the overall stability constants given directly by the programme for the input data, which include all the experimental points of all titration curves.

The stability constants for the cascade species between Cu^{2+}, $[26]py_2N_4$ and the different anions were determined from a minimum of 192 (for ox^{2-}) to 253 (for suc^{2-}) experimental points, while the association constants for the equilibrium between each anion and protonated $[26]py_2N_4$ were determined from a minimum of 135 (for fu^{2-}) to 175 (for suc^{2-}) experimental points and a minimum of two titration curves.

UV/Vis and EPR Spectrophotometric Measurements

Electronic spectra were recorded with a UNICAM model UV-4 spectrophotometer for UV/Vis, using aqueous solutions of the complexes prepared by the addition of different dicarboxylate anions (in the form of sodium or potassium salts) to the dicopper complex of $[26]py_2N_4$ at the appropriate pH value. All the solutions were prepared in the range 1.0×10^{-4} to 5×10^{-4} mol·dm^{-3}. EPR spectroscopic measurements of the $[Cu_2([26]py_2N_4)(H_2O)_4]^{4+}$ and of its cascade complexes with the different anions were recorded with a Bruker ESP 380 spectrometer equipped with continuous-flow cryostat for liquid helium, operating at X-band. The solutions were prepared at 2.0×10^{-3} mol·dm^{-3} in water/DMSO (1:1), at 6.4–11.4 K.

Molecular Modelling

The MM and MD calculations were carried out using the Universal Force Field[22] within the Cerius2[23] package software. The atomic charges were calculated with the Qeq equilibration method implemented within Cerius2. The conformational analyses of $H_4[26]py_2N_4^{4+}$ and $[Cu_2([26]py_2N_4)]^{4+}$ complexes, as well as the docking of these receptors to the anions, were undertaken thorough the quenched dynamics at 3000 K. The dynamic behaviour of the host–guest complexes was investigated by MD simulations at 300 K.

The molecular modelling studies started with conformational analysis on the $H_4[26]py_2N_4^{4+}$ receptor. The starting model was obtained from the manipulation of the X-ray atomic coordinates of a related compound. The structure was subsequently minimised and the charges recalculated, then this process was repeated successively until the steric energy remained constant. Finally, the minimised structure was heated at 3000 K over 2 ns and the snapshots were saved every 0.2 ps leading to a total of 10000 conformations, which were concomitantly minimised by MM. Subsequently the lowest energy conformation found for $H_4[26]py_2N_4^{4+}$ was docked with the anions ox^{2-}, mal^{2-}, suc^{2-} and ma^{2-} by a quench dynamics run of 500 ps. The structures of the anions were also previously minimised by MM and their charges were calculated by the Qeq equilibration method with the total charge adjusted to –2. The dynamic behaviour of each of the lowest energy arrangements found for the inclusion compounds was subsequently evaluated by MD at room temperature over 1 ns.

The starting models of $[Cu_2([26]py_2N_4)]^{4+}$ in five different conformations were obtained from manipulation of the atomic coordi-

nates retrieved from the X-ray structure of a related compound. Charges of +2 were given to the two Cu^{2+} ions and the charges on the atoms of the macrocycle were calculated independently of the metal centres by the Qeq equilibration method assuming a neutral ligand. The structures were subsequently minimised and the charges recalculated, then this process was repeated successively until the steric energy remained constant. The Cu–N bonds were retained in the calculation, being described through a theta harmonic function with ideal distances of 2.00 and 1.93 Å for Cu–Nsp^3 and Cu–Nsp^2 bonds respectively. The bending N–Cu–N angles were restrained to the ideal angles of 90 and 180° using a cosine harmonic function. Then all minimised structures were subjected to a quenching dynamics runs of 100 ps.

The study of host–guest interactions with $[Cu_2([26]py_2N_4)]^{4+}$ receptor also started with docking of its lowest + + + + conformation found on conformational analyses and the bridging anions (ox^{2-}, mal^{2-}, suc^{2-} and ma^{2-}) positioned above the macrocyclic cavity and on the same side of the N–H groups. No bonds between the donor atoms of the bridging ligands and the copper centres were considered and therefore the host–guest bonding interactions were purely electrostatic. Each starting model was subject to a MD quenching simulation of 100 ps. The dynamic behaviour of the lowest energy structures found for each cascade complex was subsequently investigated by MD simulations over 1 ns. All simulations were carried out using a constant NVE thermostat with default parameters and a time step of 1.0 fs. The events were saved at intervals of 0.1 ps, except on the conformational analysis of $[Cu_2([26]py_2N_4)]^{4+}$ where the frames were saved every 0.2 ps as stated above.

Acknowledgments

The authors acknowledge the financial support from Fundação para a Ciência e a Tecnologia (FCT) and POCTI, with co-participation of the European Community fund FEDER (Projects n. POCTI/1999/QUI/35396 and POCTI/QUI/49114/2002). The authors also acknowledge R. Mortágua and M. Pereira for assistance in the computer modelling studies and EPR experiments, respectively. F.L. also acknowledges FCT for a grant (SFRH/BD/9113/2002).

[1] C. A. Ilioudis, J. W. Steed, *J. Supramol. Chem.* **2001**, *1*, 165–187.
[2] R. J. Fitzmaurice, G. M. Kyne, D. Douheret, J. D. Kilburn, *J. Chem. Soc., Perkin Trans. 1* **2002**, 841–864.
[3] R. Martínez-Máñez, F. Sancenón, *Chem. Rev.* **2003**, *103*, 4419–4476.
[4] J. M. Llinares, D. Powell, K. Bowman-James, *Coord. Chem. Rev.* **2003**, *240*, 57–75.
[5] P. A. Gale, *Coord. Chem. Rev.* **2003**, *240*, 191–221.
[6] J. L. Sessler, P. I. Sansom, A. Andrievsky, V. Kral in *Supramolecular Chemistry of Anions* (Eds.: A. Bianchi, K. Bowman-James, E. García-España), Wiley-VCH, **1997**, pp. 355–419.
[7] V. Amendola, L. Fabbrizzi, C. Mangano, P. Pallavicini, A. Poggi, A. Taglietti, *Coord. Chem. Rev.* **2001**, *219–221*, 821–837.
[8] L. Fabbrizzi, M. Licchelli, G. Rabaioli, A. Taglietti, *Coord. Chem. Rev.* **2000**, *205*, 85–108.
[9] F. Li, R. Delgado, J. Costa, M. G. B. Drew, V. Félix, *Dalton Trans.* **2005**, 82–91.
[10] P. Gans, A. Sabatini, A. Vacca, *Talanta* **1996**, *43*, 1739–1753.
[11] L. D. Pettit, H. K. J. Powell, *IUPAC Stability Constants Database*, Academic Software, Timble, **2003**.
[12] L. Alderighi, P. Gans, A. Ienco, D. Peters, A. Sabatini, A. Vacca, *Coord. Chem. Rev.* **1999**, *184*, 311–318.
[13] L. Branco, J. Costa, R. Delgado, M. G. B. Drew, V. Félix, B. J. Goodfellow, *J. Chem. Soc., Dalton Trans.* **2002**, 3539–3550.
[14] T. G. Fawcett, E. E. Bernarducci, K. Krogh-Jespersen, H. J. Schugar, *J. Am. Chem. Soc.* **1980**, *102*, 2598–2604.
[15] K. A. Meadows, F. Liu, J. Sou, B. P. Hudson, D. R. McMillin, *Inorg. Chem.* **1993**, *32*, 2919–2923.
[16] J. Liu, T.-B. Lu, H. Li, Q.-L. Zhang, L.-N. Ji, T.-X. Zhang, L.-H. Qu, H. Zhou, *Transition Met. Chem.* **2002**, *27*, 686–690.
[17] T. Lu, X. Zhuang, Y. Li, S. Chen, *J. Am. Chem. Soc.* **2004**, *126*, 4760–4761.
[18] T. D. Smith, J. R. Pilbrow, *Coord. Chem. Rev.* **1974**, *13*, 173–278.
[19] D. M. Duggan, D. N. Hendrickson, *Inorg. Chem.* **1974**, *13*, 2929–2940.
[20] C.-L. O'Young, J. C. Dewan, H. R. Lilienthal, S. J. Lippard, *J. Am. Chem. Soc.* **1978**, *100*, 7291–7300.
[21] S. Carvalho, C. Cruz, R. Delgado, M. G. B. Drew, V. Félix, *Dalton Trans.* **2003**, 4261–4270.
[22] A. K. Rappe, C. J. Casewit, K. S. Colwell, W. A. Goddard III, W. M. Skiff, *J. Am. Chem. Soc.* **1992**, *114*, 10024–10035.
[23] *CERIUS2*, version 4.2, Molecular Simulations Inc, San Diego, **2000**.
[24] S. E. Matthews, P. Schmitt, V. Félix, M. G. B. Drew, P. D. Beer, *J. Am. Chem. Soc.* **2002**, *124*, 1341–1355.
[25] B. Dietrich, M. W. Hosseini, J. M. Lehn, R. B. Sessions, *J. Am. Chem. Soc.* **1981**, *103*, 1282–1283.
[26] M. W. Hosseini, J. M. Lehn, *J. Am. Chem. Soc.* **1982**, *104*, 3525–3527.
[27] M. W. Hosseini, J. M. Lehn, *Helv. Chim. Acta* **1986**, *69*, 587–603.
[28] R. J. Motekaitis, A. Martell, *Inorg. Chem.* **1992**, *31*, 5534–5542.
[29] Q. Lu, R. J. Motekaitis, J. Reibenspies, A. Martell, *Inorg. Chem.* **1995**, *34*, 4958–4968.
[30] C. Anda, A. Llobet, A. Martell, J. Reibenspies, E. Berni, X. Solans, *Inorg. Chem.* **2004**, *43*, 2793–2802.
[31] J. B. English, A. E. Martell, R. J. Motekaitis, I. Murase, *Inorg. Chim. Acta* **1997**, *258*, 183–192.
[32] T. F. Pauwels, W. Lippens, G. G. Herman, A. M. Goeminne, *Polyhedron* **1998**, *17*, 1715–1723.
[33] T. F. Pauwels, W. Lippens, P. W. Smet, G. G. Herman, A. M. Goeminne, *Polyhedron* **1999**, *18*, 1029–1037.
[34] G. T. S. Martins, B. Szpoganicz, V. Tomisic, N. Humbert, M. Elhabiri, A.-M. Albrecht-Gary, L. F. Sala, *Inorg. Chim. Acta* **2004**, *357*, 2261–2268.
[35] G. Shwardzenbach, W. Flaschka, *Complexometric Titrations*, Methuen & Co, London, **1969**.

Received: December 29, 2004
Published Online: October 5, 2005

